



Published in final edited form as:

Cancer. 2012 July 1; 118(13): 3433–3445. doi:10.1002/cncr.26621.

Inhibition of the NADPH oxidase regulates HO-1 expression in chronic myeloid leukemia

Melissa M. Singh, Ph.D.¹, Mary E. Irwin, Ph.D.¹, Yin Gao, Ph.D.¹, Kechen Ban, Ph.D.¹, Ping Shi, Ph.D.³, Ralph B. Arlinghaus, Ph.D.², Hesham M. Amin, M.D.³, and Joya Chandra, Ph.D.¹

¹Department of Pediatrics Research, University of Texas MD Anderson Cancer Center; 1515 Holcombe Blvd.; Houston, Texas 77030

²Department of Molecular Pathology, University of Texas MD Anderson Cancer Center; 1515 Holcombe Blvd.; Houston, Texas 77030

³Department of Hemapathology, University of Texas MD Anderson Cancer Center; 1515 Holcombe Blvd.; Houston, Texas 77030

Abstract

Background—Patients with blast crisis phase chronic myelogenous leukemia (CML) have poor response to tyrosine kinase inhibitors designed to inhibit the BCR-ABL1 oncogene. Recent work has shown that heme oxygenase 1 (HO-1) expression is increased in BCR-ABL1 expressing cells and that inhibition of HO-1 in CML leads to reduced cellular growth suggesting HO-1 may be a plausible target for therapy. Here we sought to clarify the mechanism of HO-1 overexpression and the role of the NADPH oxidase as a contributor to this mechanism in CML.

Methods—HO-1 expression was evaluated in CML bone marrow specimens from patients in various stages of disease, in a transplant based model for CML and in CML cell lines. Chemical and genetic inhibition of the NADPH oxidase was carried out in CML cells.

Results—Blast crisis CML patient specimens displayed higher levels of HO-1 staining than chronic or accelerated phase. HO-1 upregulation in BCR-ABL1 expressing cells was suppressed by diphenyliodonium (DPI), a chemical inhibitor of the NADPH oxidase. Targeting the NADPH oxidase through RNAi to Rac1, a dominant negative Rac1 construct or an inhibitor of Rac1 activity also blunted HO-1 protein expression. Moreover, inhibition of the NADPH oxidase by RNAi directed towards p47phox similarly abrogated HO-1 levels.

Conclusion—BCR-ABL1 expression upregulates HO-1, a survival factor for CML cells. This upregulation is more pronounced in blast crisis CML relative to early stage disease and is mediated by the NADPH oxidase components Rac1 and p47phox. Expression of p47phox is increased in BCR-ABL1 expressing cells.

Keywords

oncogenes; oxidative stress; BCR-ABL; HO-1; NADPH oxidase

Corresponding author: Joya Chandra, Ph.D., Department of Pediatrics Research, Box 853, 1515 Holcombe Blvd., Houston, TX 77030, jchandra@mdanderson.org, Phone: 713-563-5405, FAX: 713-563-9607.

Financial Disclosures: There are no financial disclosures from any of the authors.

Introduction

Molecular details of the BCR-ABL1 oncogene's effects in chronic myelogenous leukemia (CML) cells have enabled the development of an armamentarium of effective new therapies which are primarily kinase inhibitors¹. While these strategies are very effective at combating chronic phase disease, patients with blast crisis CML are often resistant to kinase inhibitors and can be offered few effective therapies². Therefore, investigation of molecular alterations associated with blast crisis CML will aid in the development of better treatments.

In addition to functioning as a kinase, BCR-ABL1 increases levels of intracellular reactive oxygen species (ROS)³, a feature which has been linked to DNA damage and secondary mutations seen in blast crisis CML^{4, 5}. However, the source of increased ROS in BCR-ABL1 expressing cells is poorly understood. Endogenous sources of oxidative stress include the activation of ROS-producing complexes such as the NADPH oxidase. There are five Nox isoforms, termed Nox1-5, and two related enzymes, DUOX1 and DUOX2. Each of these enzymes consists of a unique combination of subunits, which include p47phox, p67phox, p22phox, NoxO1, NoxA1 and Rac1, for activity. Initial studies of the NADPH oxidase focused on Nox2 in myeloid cells, which requires assembly of p22phox, p47phox, p67phox and Rac1 for activation of the oxidase. Once assembled, the oxidase produces a superoxide burst that serves as a defense mechanism to counter bacterial attacks. Currently, few studies have addressed the relationship between BCR-ABL1 and the NADPH oxidase. Interestingly, CML patient samples and cell lines also express high levels of Nox2⁶ which may cause the increase in intracellular ROS observed in BCR-ABL1 expressing cells. Moreover, subsequent work has revealed that numerous cell types express the NADPH oxidase which, in non-immune cells, promotes proliferation.

Regardless of the source, in virtually every cell type, elevated ROS levels are offset by upregulation of antioxidant proteins. In BCR-ABL1 expressing cells, one of these antioxidant proteins is heme oxygenase-1 (HO-1), a small heat shock protein, also known as hsp32⁷. HO-1 belongs to a family of heme oxygenases consisting of two active isoforms, HO-1 and HO-2. These enzymes primarily function in the degradation of heme to biliverdin, a compound with antioxidant properties⁸. While HO-1 is known to be inducible by oxidative stress, such as that caused by BCR-ABL1, HO-2 is constitutively expressed and is not further induced by stress. A third isoform, HO-3, shares sequence similarity but does not seem to be catalytically active^{9, 10}. Like other small heat shock protein family members, HO-1 possesses anti-apoptotic properties. Recent work has linked its expression to survival of myeloid cells and to drug resistance¹¹.

In the current study, we evaluated CML patient specimens from various stages of progression, a CML mouse model and various CML cell lines for HO-1 expression and report increased HO-1 in blast crisis bone marrow specimens. Interestingly, BCR-ABL1 expressing cells possess higher levels of p47phox providing a plausible mechanism for elevated ROS and HO-1 expression by BCR-ABL1. We provide evidence, using chemical, mutational, and RNAi based applications, that HO-1 expression is regulated by the NADPH oxidase components, Rac1 and p47phox, in CML. Therefore our data points to a novel pathway linking BCR-ABL1 to the NADPH oxidase and HO-1, highlighting new opportunities for therapeutic intervention for blast crisis CML.

Materials and Methods

Cells, chemicals and antibodies

Parental K562 cell lines were obtained from American Type Culture Collection (Manassas, VA), imatinib resistant K562 cells were kindly provided by Dr. James Griffin (Dana Farber

Cancer Institute, Harvard Medical Center, MA), BaF3 cells transduced with empty vector, p210 BCR-ABL1 or mutant BCR-ABL1 were kindly provided by Dr. Charles Sawyers (Memorial Sloan Kettering Cancer Center, NY), and TonBp210 cells were kindly provided by Dr. George Daley (Children's Hospital Boston, Harvard Medical School, MA). N-acetylcysteine (NAC), diphenyliodonium chloride (DPI), rotenone, and wortmannin were purchased from Sigma (St. Louis, MO). The Rac1 inhibitor NSC23766 was purchased from EMD4Biosciences. Antibodies used in this study were obtained from the following: HO-1, Enzo Life Sciences (Farmingdale, NY); β -actin, Sigma (St. Louis, MO); p210 BCR-ABL1 (8E9), gift from Dr. Ralph Arlinghaus (MD Anderson Cancer Center, Houston, TX); Rac1, Millipore (Billerica, MA); myc and p47phox, Santa Cruz Biotechnology (Santa Cruz, CA).

Immunohistochemistry of CML Tissue Microarray

Patient specimens were used for this study and were collected after informed consent was obtained in accordance with the Declaration of Helsinki. Tissue microarray studies were initiated after approval from the University of Texas M.D. Anderson Cancer Center (UTMDACC) Institutional Review Board. The tissue microarray contained bone marrow specimens from 10 chronic-phase patients, 8 accelerated-phase patients, and 17 blastic-phase patients, spotted in triplicate. Tissue sections (4 μ m thick) were deparaffinized in xylene and rehydrated by using a graded ethanol series. Heat-induced epitope retrieval was performed with Tris-HCl buffer (pH 8.0). 3,3'-diaminobenzidine/H₂O₂ (Biogenex, San Ramon, CA) and chromogen with hematoxylin was used as the counterstain. HO-1 protein expression was evaluated in the specimens using a HO-1 specific antibody and the patients with >20% HO-1-positively stained cells was considered significant.

Detection of mRNA and protein for HO-1 in murine CML transplant model

A CML mouse transplant model, approved by the UTMDACC Institutional Animal Care and Use Committee, was set up as described previously¹². Briefly, marrow cells were harvested from C57/Bl6 mice injected with 200 mg/kg 5-fluorouracil and infected with virus harboring MigR1 p210 BCR-ABL1. Virus infected cells were injected into the tail vein of irradiated (600 cGy) recipient mice. After 14 days, marrow cells from the recipient mouse were sorted based upon GFP positivity and total RNA was isolated using Trizol reagent (Invitrogen, Carlsbad, CA) according to the manufacturer's instructions. RT-PCR was performed to amplify HO-1 using the following primers: FAACAAGCAGAACCCAGTCTA and R-CCTTCTGTGCAATCTTCTTC. Transplant efficiency was verified by BCR-ABL1 and β -actin amplification. For HO-1 and β -actin, PCR conditions included 40 cycles with an annealing temperature of 57°C, and for BCR-ABL1 60 cycles with an annealing temperature of 55°C.

Quantification of ROS

CM-H₂DCF-DA (Molecular Probes/Invitrogen, Carlsbad, CA) was used to assay intracellular ROS levels as previously described¹². Briefly, cells were collected by centrifugation after exposure to NAC, DPI, wortmannin, rotenone or diluent at the concentration and duration indicated and resuspended in phosphate-buffered saline (PBS) containing 10 μ M CM-H₂DCF-DA. Samples were incubated for 30 minutes in the dark at 37°C, washed with PBS to remove unreacted dye, read on the FL-1 channel of a Becton Dickinson FACSCalibur, and analyzed using CellQuest Software (Becton Dickinson, Franklin Lakes, NJ).

Knockdown of Rac1 and p47phox or overexpression of dominant negative Rac1

The following sequences targeting mouse Rac1 were cloned into the pSuperior retro.neo +gfp vector (Oligoengine, Seattle, WA) according to the manufacturer's protocol: Rac1-1:

5'GACGGAGCTGTTGGTAAAA-3', Rac1-2: 5'GAGAACACCTAAGCACTAA-3', Rac1-3: 5'-GCGTTGAGTCCATATTTAA-3', Rac1-4: 5'-GCAACTAGGTGTGCAAATC-3'. p47phox siRNA was purchased from Santa Cruz Biotechnology (Santa Cruz, CA). The dominant negative Rac1 construct, Rac1N.17-myc, was purchased from Addgene (Cambridge, MA). Plasmids (2 µg) or siRNA (2 µM) were introduced into 2×10^6 BaF3-p210 cells by nucleofection (Lonza Group Ltd., Basel, Switzerland) using program X-01.

Western blotting

HO-1, BCR-ABL1, Rac1, and p47phox protein expression was monitored in total cell lysates prepared using Triton X-100 buffer (PBS with 1% Triton X-100, 25 mM Tris, pH 7.5, and 150 mM NaCl) containing protease inhibitor cocktail (Roche). Proteins were separated by SDS-PAGE and detected by Western blot analysis using designated antibodies listed above at 1:1000 dilution. Immunoreactive bands were visualized using corresponding HRP conjugated secondary antibodies followed by chemiluminescent detection (GE Healthcare, Waukesha, WI). The intensity of the bands was measured and analyzed using Image J software.

Cellular proliferation and viability analyses

BaF3 cells transduced with BCR-ABL1 (p210) or vector were plated at a density of 0.5×10^6 cells per mL and then treated with increasing doses (25-1000 µM) of NSC23766 for 24 hours. Cell viability was analyzed by diluting cellular suspension 1:1 in trypan blue and counting positive cells by hemocytometry. Cellular proliferation was performed on K562 cells which were plated at a density of 0.25×10^6 cells per mL and treated with increasing doses of diphenylene iodonium (DPI; 0.5-30 µM) or NSC23766 (25-1000 µM) for 24 hours. Viable cell numbers were determined by counting with a hemocytometer. IC₅₀ concentrations were determined by fitting non-sigmoidal dose response curves in GraphPad Prism software. K562 cells were then plated at a density of 0.25×10^6 cells per mL and treated for 48 hours with 125 or 250 nM imatinib alone, or in combination with the IC₅₀ dose of NSC23766 (89.9 µM). Cells were then centrifuged, washed with PBS, and incubated with propidium iodide solution (50 µg/mL PI, 0.1% Triton X-100, and 0.1% sodium citrate in PBS) for 4 h at 4°C. DNA fragmentation was quantified by flow cytometry on the FL-3 channel (FACSCalibur, Becton, Dickinson, Franklin Lakes NJ). CellQuest software was used for the analysis of sub-diploid populations (BD Bioscience, Franklin Lakes NJ).

Results

HO-1 expression is increased in blastic phase CML patient specimens and in a transplant based CML mouse model

Increased expression of HO-1 has been reported in CML cell lines¹³ and an array of patient specimens. Here we assessed HO-1 expression in the three stages of CML disease; chronic, accelerated, and blastic. To address the expression of HO-1 through progression of CML, we employed a CML tissue microarray containing 35 samples from patients progressing from chronic, accelerated, and ultimately blast crisis phase of disease and conducted immunohistochemistry for HO-1. This same cohort of patients has been previously utilized to show phase specific alterations in Fyn¹⁴, which is also dependent upon regulation by oxidative-stress and BCR-ABL1. From this array, two representative cases of HO-1 staining in chronic phase and upon progression of the same patient to blastic phase are shown in Fig. 1A. In both examples, there is little baseline expression of HO-1 protein. With progression to blast crisis, however, a dramatic increase in HO-1 staining is evident. In a panel of patients in various stages of disease, the amount of HO-1 positivity was quantified by phase

of disease and is depicted graphically (Fig. 1B). Only 20% of the chronic phase specimens showed significant staining (with greater than 20% of the cells positive) for HO-1. In contrast, 80% of the blastic phase patients demonstrated significant positivity for HO-1 (Fig. 1B). Among the blastic phase patients positive for HO-1 staining, 6 specimens were myeloid and 6 were lymphoid in origin and equal numbers of myeloid and lymphoid specimens stained negative for HO-1 expression (Table 1). This indicates that there is no difference in the level of HO-1 expression between lymphoid and myeloid blast crisis samples. In addition, there is no clear correlation linking additional cytogenetic abnormalities with HO-1 expression level (Table 1). These data indicate that HO-1 protein upregulation is associated with progression to blastic phase in both lymphoid and myeloid disease.

To extrapolate these findings to a well established transplant based mouse model for CML¹², bone marrow from donor mice was infected with retrovirus expressing MigR1-GFP-p210 and injected intravenously into irradiated recipient mice. Peripheral blood cells were sorted and RNA isolated from GFP- and GFP+ cells. Comparison of HO-1 mRNA in GFP- and GFP+ indicated that GFP+ cells expressing BCR-ABL1 had higher levels of HO-1 (Fig. 1C).

HO-1 protein expression is increased in multiple cell line models for CML

We next explored whether a specific degree of increased expression of BCR-ABL1 was required for upregulating HO-1. TonB cells transfected with a tetracycline inducible BCR-ABL1 expression system (Fig. 2A) were used to incrementally increase expression of the oncogene. Upon induction of BCR-ABL1 with 1 μ g/ml doxycycline over 12, 24, 36 and 48 h, HO-1 expression was increased. However, HO-1 expression reached a plateau by 12 h whereas BCR-ABL1 protein continued to increase over time, suggesting that HO-1 levels may be kept in check by other mechanisms. Protein expression of HO-1 was also heightened in a human CML cell line originally isolated from a patient in blast crisis, K562, and its imatinib resistant counterpart (K562-STI). An additional model for BCR-ABL1 expression was evaluated: the hematopoietic cell line BaF3, transduced with either vector, wildtype BCR-ABL1 or two imatinib resistant mutations of BCR-ABL1 (E255K or T315I) (Fig. 2B). In all of these systems, HO-1 expression is higher in cells that express BCR-ABL1, regardless of mutation status. These data suggest that HO-1 expression is a feature of all BCR-ABL expressing cells, even those that are imatinib resistant.

Chemical inhibitors of ROS or of the NADPH oxidase reduce expression of HO-1 in CML cells

Since HO-1 is responsive to oxidative stress¹⁵⁻¹⁸, we tested the effects of blocking ROS on HO-1 expression. K562 cells were treated for 24 h with either diluent, a general antioxidant, NAC, or a NADPH oxidase-specific inhibitor, DPI¹⁹ to first confirm that these compounds reduced ROS levels in BCR-ABL1 expressing cells. After exposure to DPI, intracellular peroxide levels are reduced by a log as measured by mean fluorescence intensity in K562 cells (Fig. 3A). Exposure to either NAC or DPI caused a decrease in HO-1 levels (Figure 3B), which reinforces the oxidant dependence of HO-1 upregulation and implicates the NADPH oxidase as a potential contributor to HO-1 expression.

Chemical inhibition of the NADPH oxidase suppresses ROS more effectively than inhibition of electron transport or Akt signaling in BCR-ABL1 expressing cells

The NADPH oxidase is one of many endogenous sources of oxidative stress that normally function in the cell²⁰. Previously, the NADPH oxidase, as well as other sources of ROS have been linked to BCR-ABL1, and have been attributed to the increase in oxidative stress seen in these cells^{21, 22}. In BaF3-p210 cells, we compared an inhibitor of mitochondrial respiration, rotenone, and an inhibitor of Akt signaling, wortmannin, to the effect of DPI on

intracellular peroxide levels. Figure 4 shows that DPI was more effective than either previously reported regulators of BCR-ABL1-induced oxidative stress. A representative histogram comparing effects of DPI to doses and exposures of wortmannin and rotenone previously published as lowering ROS in BCR-ABL1 expressing cells is shown in Figure 4A. Figure 4B is a summary of three experiments in which DCF fluorescence (indicative of intracellular peroxide levels) was quantified. A significant reduction ($p = 0.01$) of ROS in BCR-ABL1 expressing cells was noted upon exposure to DPI (Figure 4B). Collectively, these data reinforce the notion that chemical inhibition of the NADPH oxidase by DPI impacts ROS levels more so than inhibitors of mitochondrial respiration or Akt signaling.

Rac1 and p47phox, both components of the NADPH oxidase, contribute to protein expression of HO-1 in CML cells

Decreased ROS production upon treatment with DPI suggests involvement of at least one of the Nox enzymes. Previous studies have identified Nox4 as a contributor to the elevated ROS observed upon induction of BCR-ABL1²¹. Interestingly, we found that one of the subunits of Nox2, p47phox²³, was increased by 2.5 fold in BCR-ABL1 expressing cells as compared to vector control cells (Figure 4C). Since DPI is reported to inhibit other flavoproteins in addition to the NADPH oxidase, we set out to more specifically implicate Nox2 by targeting individual components of this multi-protein complex. Rac1 is a crucial component of several of the NADPH oxidase enzymes²⁰, including Nox2, and serves to activate other cytosolic subunits of the oxidase (p47phox, p67phox, and p40phox) and congregates at the cell surface interface to form the active oxidase. We first targeted Rac1 by employing shRNA directed towards Rac1 to knockdown protein expression (Fig. 5A) in BaF3-p210 cells. Several different sequences were used to knockdown Rac1 with some sequences being more or less effective than others. In general, Rac1 knockdown correlated with decreased expression of HO-1. A Rac1 shRNA that suppressed nearly 60% of Rac1 expression also suppressed HO-1 expression by nearly 70% (Fig. 5A, Lane 5). We also blocked Rac1 activity by two additional approaches: transfection of a dominant negative mutant of Rac1, N.17-myc (Fig. 5B) and by treating cells with a chemical inhibitor of Rac1, NSC23766 (Fig. 5C). Both approaches suppressed HO-1 protein expression, however, the dominant negative approach was more effective at blunting HO-1 expression, achieving a 50% reduction in levels than the small molecule which diminished HO-1 by 30% at the highest concentration used. Nonetheless, these three strategies used to modulate Rac1 activity indicate it is critical for maintenance of HO-1 levels in BCR-ABL1 expressing cells.

Since Rac1 is required for the activation of several of the Nox enzymes, we knocked down p47phox (Fig. 5D), a subunit specific for Nox2, and evaluated protein expression of HO-1. Similar to our results obtained with Rac1 inhibition, knockdown of p47phox also suppressed HO-1 protein expression by 50%, thereby implicating two NADPH oxidase components (Rac1 and p47phox) in controlling HO-1. These results indicate that the NADPH oxidase leads to the increase in ROS observed in BCR-ABL1 expressing cells and that inhibition of the oxidase modulates the levels of HO-1, providing an additional therapeutic target for the treatment of CML.

Combination of inhibitors targeting Nox and BCR-ABL1 enhance cell death in CML cells

To assess the selectivity of Rac1 inhibition for therapy of BCR-ABL1 positive malignancies, we treated BaF3 cells transduced with vector or BCR-ABL1 with increasing doses of NSC23766 for 24 hours and evaluated cell viability (Figure 6A). All doses of the Rac1 inhibitor used resulted in a greater loss of viability, as measured by trypan blue positivity, in BCR-ABL1 expressing cells as compared to the vector controls (Figure 6A). In addition, both chemical inhibition of Rac1 in K562 blast crisis CML cells and the inhibition of Nox

by DPI inhibit proliferation (Figure 6B) within the same range of drug that affects HO-1 expression (Figure 3B and 5C).

Our results demonstrate that targeting Nox2 via Rac1 inhibition or DPI may be a viable therapeutic option to induce cell death and affect proliferation of CML. Therefore, we asked whether inhibition of Nox2 in combination with imatinib cooperate to enhance cell death. In order to evaluate this hypothesis, we treated K562 cells with the calculated IC₅₀ value for NSC23766 (89.9 μ M; data not shown) with or without 125 nM or 250 nM imatinib for 48 hours and measured DNA fragmentation by PI staining (Figure 6C). As depicted in Figure 6C, imatinib alone did not significantly influence DNA fragmentation at these doses although higher doses effectively caused DNA fragmentation (data not shown). However, combined treatment of K562 cells with NSC23766 and imatinib led to a dramatic increase in DNA fragmentation as compared to either NSC23766 or imatinib alone (Figure 6C). These results indicate that use of NSC23766 in combination with imatinib augments the induction of DNA fragmentation. Taken together, these data provide evidence to suggest that targeting Rac1 or Nox is selective for CML and combined inhibition of Nox with imatinib may be a novel therapeutic option for the treatment of CML.

Discussion

The present study shows that the NADPH oxidase, specifically Nox2, is a major contributor to HO-1 upregulation, which is a feature of CML blast crisis. As depicted in Figure 7, RNAi directed towards either Rac1 or p47phox blunts HO-1 expression indicating that these two components of the oxidase are regulators of HO-1. Since HO-1 has been implicated in cell survival, targeting the NADPH oxidase is a novel way to target this anti-oxidant and anti-apoptotic protein. Direct targeting of HO-1 using siRNA and pharmacological inhibitors has been reported to induce apoptosis in cells expressing wildtype and imatinib resistant mutant BCR-ABL1^{11, 13}. However, the pharmacological inhibitors used were water soluble, cell permeable conjugates of zinc protoporphyrin (ZnPP) which theoretically could target any Fe containing compound. Another drawback of ZnPP is that it may actually modulate heme levels²⁴, which may have broad pleotropic effects. The same group reported that induction of HO-1 using hemin protected cells from imatinib cytotoxicity. In fact, our studies demonstrate that reducing HO-1 expression, via a Rac1 inhibitor, sensitizes BCR-ABL1 expressing cells to imatinib (Figure 6). These data further support the concept that HO-1 inhibition (either directly or indirectly) is a potentially therapeutically viable goal. Given our data showing increased expression of HO-1 in blast crisis CML, this patient population stands to benefit most from the development of such strategies.

While inhibition of HO-1 in CML appears warranted by our results, as with any new therapy, evaluation of toxicities will be required. In particular, induction of HO-1 displays cytoprotective and anti-inflammatory properties in cardiac, hepatic, and renal tissues when oxidative stress is elevated. For example, in settings of ischemia-reperfusion injury, which leads to significant elevation of ROS after reoxygenation, induction of HO-1 is protective²⁵. However, in cancer, HO-1 expression is more highly expressed in a variety of tumor types (²⁶ and Figure 1) as compared to surrounding normal tissue. Also, our data (Figure 6A) demonstrates that inhibition of Rac1, which influences HO-1 expression (Figure 5), is selective for cells that express BCR-ABL1.

As a small heat shock protein, HO-1 is known to be inducible by oxidative stress as an adaptive response⁷. In addition to functioning as a potent kinase, a feature of the BCR-ABL1 oncogene is its ability to raise levels of intracellular ROS³. In BCR-ABL1 expressing cells, blocking ROS levels with NAC also blocks HO-1 protein expression, indicating that BCR-ABL1 mediated ROS contribute to expression of this pro-survival protein. More

broadly, oxidative stress in CML as a consequence of the BCR-ABL1 oncogene has been linked to DNA damage and altered DNA repair capacity^{4, 5, 27}. Specifically, 32Dcl3 cells overexpressing BCR-ABL1 contain higher levels of DNA damage than vector transfectants as measured by the Comet assay⁵. Another report shows that lower DNA repair capacity²⁷ in BCR-ABL1 expressing cells causes point mutations which may account for the many secondary mutations seen in blast crisis. *In vivo* experiments support this concept⁴: SCID mice were fed a Vitamin E rich diet for a week prior to being reconstituted with BCR-ABL1 transduced 32D cells and was continued through and post injection of CML cells. Mononuclear cells from these mice had a lower rate of point mutations seen in blast crisis. Taken together, these data link BCR-ABL1-initiated ROS to features of blast crisis CML. Our results indicate that increased expression of HO-1 protein is yet another ROS dependent molecular feature of progressed CML cases.

Given the relationship between oxidative stress and blast crisis CML, understanding the molecular events that lead to heightened ROS in BCR-ABL1 expressing cells has potential therapeutic impact. Prior work has attributed oxidative stress in BCR-ABL1 transformed cells to higher generation of ROS by electron transport and increased PI3K signaling²². We compared inhibition of these ROS sources to inhibition of the NADPH oxidase and found that the latter had a far more significant effect on intracellular ROS levels in BCR-ABL1 expressing cells. Therefore, targeting the NADPH oxidase may represent a novel way to prevent features of progression to blast crisis, inclusive of, but not limited to upregulation of HO-1. We find that p47phox protein is overexpressed in cells constitutively expressing BCR-ABL1 and that targeting p47phox or Rac1 leads to reduced HO-1 expression. Since Nox2 is the only Nox isoform that requires both p47phox and Rac1, our data suggest that Nox2 is important in the mechanism of elevated ROS and subsequent changes in HO-1 observed in these cells. While Nox2 is expressed in other cell models for CML, knockdown studies using an inducible system for BCR-ABL1 expression show that Nox4 plays a major role in BCR-ABL1 induced ROS²¹. In contrast, in patient derived KU812 cells, neither Nox2 nor Nox4 appear to be required for elevated ROS²⁸. These differences in the dependence of the specific NADPH oxidase complexes in the generation of excess ROS may be attributed to temporal effects of BCR-ABL1 expression; acute (inducible TonB.p210) vs. chronic (BaF3/p210 or KU812), or other genetic abnormalities that are present in these cell models. Regardless of whether the NADPH oxidase leads to elevated ROS, targeting the oxidase in all systems leads to decreased cell survival making the oxidase a viable target for CML.

In support of targeting the NADPH oxidase in CML, the potential efficacy and feasibility of Rac1 (a NADPH oxidase component) inhibition has been addressed in an elegant study using genetic and chemical means^{29, 30}. In mice deficient in Rac1 and Rac2, expression of BCR-ABL1 by transplant of transduced marrow cells showed significantly slower myeloid disease development compared to wild type mice transplanted with BCR-ABL1 transduced marrow. These investigators also used the same small molecule antagonist of Rac activation used in Figure 5C, NSC23766, to inhibit clonogenic growth of CML patient derived bone marrow cells and to show *in vivo* efficacy in a mouse CML model²⁹. However, these results potentially implicate both NADPH oxidase-dependent and -independent functions of Rac1. While we cannot rule out a role for NADPH oxidase independent functions for Rac1 in CML progression, our finding that p47phox is upregulated in BCR-ABL1 expressing cells provides impetus for further study of Nox2 in CML blast crisis.

Taken together, our findings link the NADPH oxidase to HO-1 expression as depicted in Figure 7 and provide molecular insight into blast crisis CML. We demonstrate that p47phox is overexpressed in BCR-ABL1 expressing cells. A mechanistic explanation for this observation is currently underway. We posit that the upregulation of p47phox affects the

activity of Nox2 which leads to the increased ROS and a subsequent increase in HO-1 protein. Our data show that decreasing intracellular ROS, by using a general antioxidant (NAC) or an NADPH oxidase specific inhibitor (DPI), reduces the expression of HO-1. Similarly, HO-1 protein levels are diminished when the NADPH oxidase is more specifically targeting using knocking down strategies directed towards p47phox or Rac1. Moreover, dominant negative and chemical means for targeting Rac1 also decrease HO-1 protein expression. Collectively, these data prompt the clinical development of direct or indirect inhibitors of the Nox2 and/or HO-1.

Acknowledgments

Funding: This work was supported by NIH R01 CA115811 (to J.C.)

References

1. Druker BJ. Translation of the Philadelphia chromosome into therapy for CML. *Blood*. 2008; 112:4808–4817. [PubMed: 19064740]
2. Quintas-Cardama A, Cortes J. Molecular biology of bcr-abl1-positive chronic myeloid leukemia. *Blood*. 2009; 113:1619–1630. [PubMed: 18827185]
3. Sattler M, Verma S, Shrikhande G, et al. The BCR/ABL tyrosine kinase induces production of reactive oxygen species in hematopoietic cells. *J Biol Chem*. 2000; 275:24273–24278. [PubMed: 10833515]
4. Koptyra M, Falinski R, Nowicki MO, et al. BCR/ABL kinase induces self-mutagenesis via reactive oxygen species to encode imatinib resistance. *Blood*. 2006
5. Nowicki MO, Falinski R, Koptyra M, et al. BCR/ABL oncogenic kinase promotes unfaithful repair of the reactive oxygen species-dependent DNA double-strand breaks. *Blood*. 2004; 104:3746–3753. [PubMed: 15304390]
6. Juhasz A, Ge Y, Markel S, et al. Expression of NADPH oxidase homologues and accessory genes in human cancer cell lines, tumours and adjacent normal tissues. *Free Radic Res*. 2009; 43:523–532. [PubMed: 19431059]
7. Mancuso C, Barone E. The heme oxygenase/biliverdin reductase pathway in drug research and development. *Curr Drug Metab*. 2009; 10:579–594. [PubMed: 19702533]
8. Tenhunen R, Marver HS, Schmid R. The enzymatic conversion of heme to bilirubin by microsomal heme oxygenase. *Proc Natl Acad Sci U S A*. 1968; 61:748–755. [PubMed: 4386763]
9. Hayashi S, Omata Y, Sakamoto H, et al. Characterization of rat heme oxygenase-3 gene. Implication of processed pseudogenes derived from heme oxygenase-2 gene. *Gene*. 2004; 336:241–250. [PubMed: 15246535]
10. McCoubrey WK Jr, Huang TJ, Maines MD. Isolation and characterization of a cDNA from the rat brain that encodes hemoprotein heme oxygenase-3. *Eur J Biochem*. 1997; 247:725–732. [PubMed: 9266719]
11. Mayerhofer M, Gleixner KV, Mayerhofer J, et al. Targeting of heat shock protein 32 (Hsp32)/heme oxygenase-1 (HO-1) in leukemic cells in chronic myeloid leukemia: a novel approach to overcome resistance against imatinib. *Blood*. 2008; 111:2200–2210. [PubMed: 18024796]
12. Pear WS, Miller JP, Xu L, et al. Efficient and rapid induction of a chronic myelogenous leukemia-like myeloproliferative disease in mice receiving P210 bcr/abl-transduced bone marrow. *Blood*. 1998; 92:3780–3792. [PubMed: 9808572]
13. Mayerhofer M, Florian S, Krauth MT, et al. Identification of heme oxygenase-1 as a novel BCR/ABL-dependent survival factor in chronic myeloid leukemia. *Cancer Res*. 2004; 64:3148–3154. [PubMed: 15126353]
14. Ban K, Gao Y, Amin HM, et al. BCR-ABL1 mediates up-regulation of Fyn in chronic myelogenous leukemia. *Blood*. 2008; 111:2904–2908. [PubMed: 18180382]
15. Alam J, Cai J, Smith A. Isolation and characterization of the mouse heme oxygenase-1 gene. Distal 5' sequences are required for induction by heme or heavy metals. *J Biol Chem*. 1994; 269:1001–1009. [PubMed: 8288554]

16. Farombi EO, Surh YJ. Heme oxygenase-1 as a potential therapeutic target for hepatoprotection. *J Biochem Mol Biol.* 2006; 39:479–491. [PubMed: 17002867]
17. Ozono R. New biotechnological methods to reduce oxidative stress in the cardiovascular system: focusing on the Bach1/heme oxygenase-1 pathway. *Curr Pharm Biotechnol.* 2006; 7:87–93. [PubMed: 16724942]
18. Ryter SW, Alam J, Choi AM. Heme oxygenase-1/carbon monoxide: from basic science to therapeutic applications. *Physiol Rev.* 2006; 86:583–650. [PubMed: 16601269]
19. Geiszt M. NADPH oxidases: new kids on the block. *Cardiovasc Res.* 2006; 71:289–299. [PubMed: 16765921]
20. Brown DI, Griendling KK. Nox proteins in signal transduction. *Free Radic Biol Med.* 2009; 47:1239–1253. [PubMed: 19628035]
21. Naughton R, Quiney C, Turner SD, Cotter TG. Bcr-Abl-mediated redox regulation of the PI3K/AKT pathway. *Leukemia.* 2009; 23:1432–1440. [PubMed: 19295548]
22. Kim JH, Chu SC, Gramlich JL, et al. Activation of the PI3K/mTOR pathway by BCR-ABL contributes to increased production of reactive oxygen species. *Blood.* 2005; 105:1717–1723. [PubMed: 15486067]
23. El-Benna J, Dang PM, Gougerot-Pocidallo MA, Marie JC, Braut-Boucher F. p47phox, the phagocyte NADPH oxidase/NOX2 organizer: structure, phosphorylation and implication in diseases. *Exp Mol Med.* 2009; 41:217–225. [PubMed: 19372727]
24. Tsiftoglou AS, Tsamadou AI, Papadopoulou LC. Heme as key regulator of major mammalian cellular functions: molecular, cellular, and pharmacological aspects. *Pharmacol Ther.* 2006; 111:327–345. [PubMed: 16513178]
25. Yamaguchi T, Terakado M, Horio F, Aoki K, Tanaka M, Nakajima H. Role of bilirubin as an antioxidant in an ischemia-reperfusion of rat liver and induction of heme oxygenase. *Biochem Biophys Res Commun.* 1996; 223:129–135. [PubMed: 8660358]
26. Was H, Dulak J, Jozkowicz A. Heme oxygenase-1 in tumor biology and therapy. *Curr Drug Targets.* 11:1551–1570. [PubMed: 20704546]
27. Dierov J, Dierova R, Carroll M. BCR/ABL translocates to the nucleus and disrupts an ATR-dependent intra-S phase checkpoint. *Cancer Cell.* 2004; 5:275–285. [PubMed: 15050919]
28. Reddy MM, Fernandes MS, Salgia R, Levine RL, Griffin JD, Sattler M. NADPH oxidases regulate cell growth and migration in myeloid cells transformed by oncogenic tyrosine kinases. *Leukemia.* 2011; 25:281–289. [PubMed: 21072051]
29. Thomas EK, Cancelas JA, Chae HD, et al. Rac guanosine triphosphatases represent integrating molecular therapeutic targets for BCR-ABL-induced myeloproliferative disease. *Cancer Cell.* 2007; 12:467–478. [PubMed: 17996650]
30. Thomas EK, Cancelas JA, Zheng Y, Williams DA. Rac GTPases as key regulators of p210-BCR-ABL-dependent leukemogenesis. *Leukemia.* 2008; 22:898–904. [PubMed: 18354486]

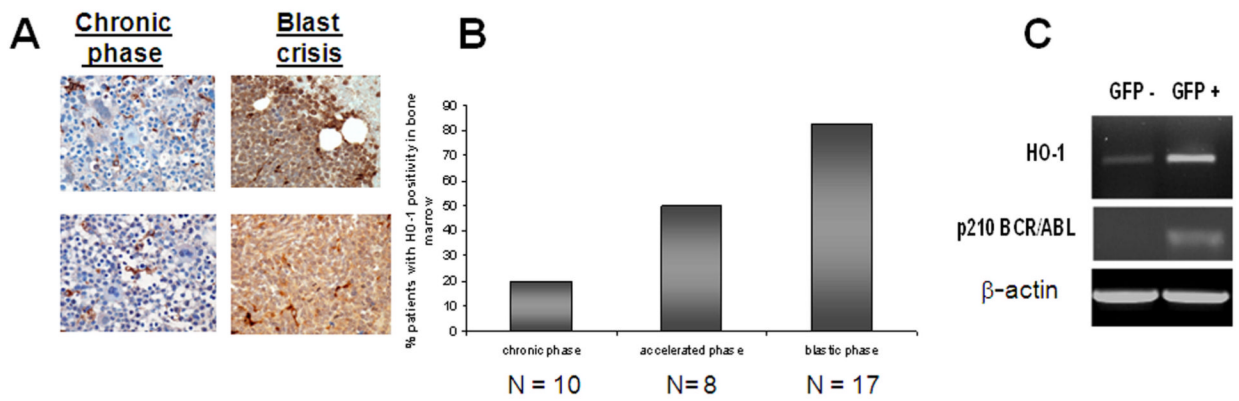


Figure 1. HO-1 expression is BCR-ABL1-dependent in vivo and is heightened in CML blast crisis specimens

(A). HO-1 protein expression is increased in blast-crisis CML. A tissue microarray containing bone marrow specimens from 10 chronic-phase patients, 8 accelerated-phase patients, and 17 blastic-phase patients, were stained using a HO-1 specific antibody. Two representative patients who were followed from chronic phase to blastic phase are shown in A. (B) Graphical representation of the percentage of patients with a significant number (>20% positive) of HO-1-positive cells. (C) HO-1 mRNA is upregulated in an animal model for CML. HO-1 mRNA expression was examined by qualitative RT-PCR using HO-1-specific primers in GFP-sorted cells from a recipient mouse transplanted with MigR1-GFP-BCR-ABL1 transduced bone marrow from a donor mouse. Transplant efficiency was verified by BCR-ABL1 and β -actin amplification.

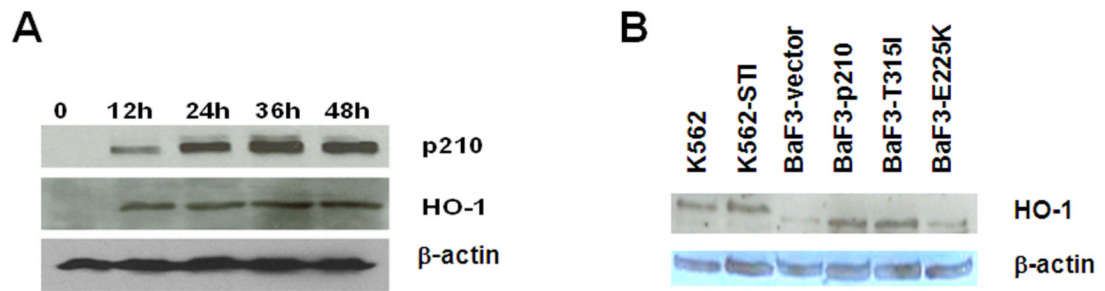


Figure 2. HO-1 expression is BCR-ABL1-dependent in vitro

(A) HO-1 protein is upregulated in TonB cells expressing BCR-ABL1 protein. TonB210 cells stably expressing a tetracycline inducible BCR-ABL1 expression vector were treated with 1 μ g/mL doxycycline for 12 h, 24 h, 36 h, or 48 h and p210 BCR-ABL1 and HO-1 protein expression was monitored by Western blot. β -actin was used as a loading control. (B) HO-1 is upregulated in imatinib sensitive and imatinib resistant CML cell lines. HO-1 protein expression was examined by Western blotting in imatinib sensitive K562 cells and BCR-ABL1 mutation independent imatinib resistant K562 cells (K562-STI) and in BaF3 cells transduced with empty vector, wild type BCR-ABL1 (BaF3-p210) or the T315I or E255K imatinib resistant mutant forms of BCR-ABL1 (BaF3-T315I; BaF3-E255K, respectively). Images shown are representative of three independent experiments.

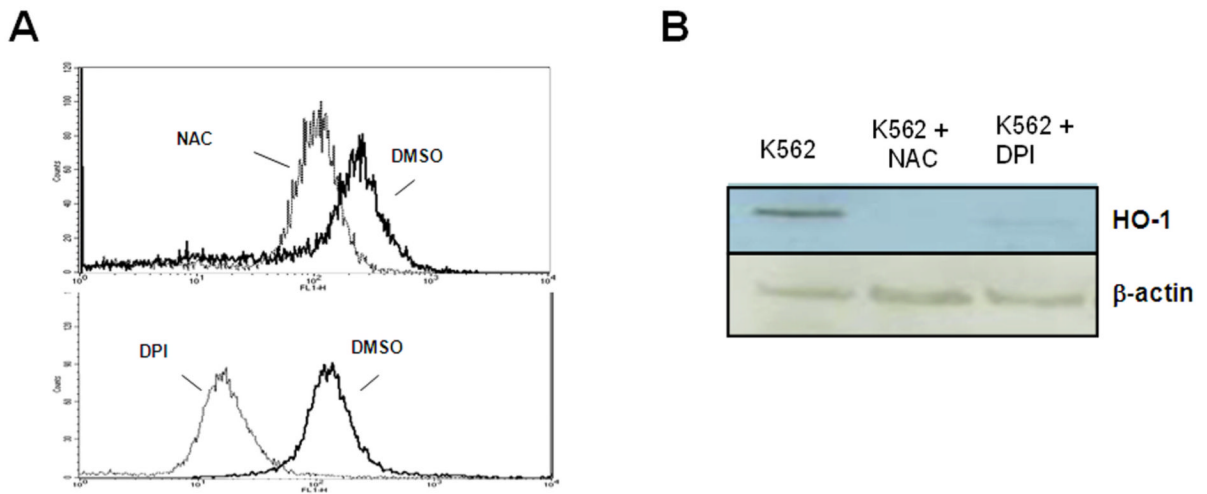


Figure 3. Inhibition of ROS diminishes HO-1 protein expression

(A) Lower levels of intracellular peroxides in K562 cells treated with NAC or DPI. Histogram representation of flow cytometric data of DCF fluorescence, indicating intracellular peroxide levels, after treatment with 24 mM NAC (upper histogram) or 30 μ M DPI (lower histogram). (B) ROS blockade using NAC or diphenylene iodonium (DPI; a NADPH oxidase inhibitor) causes a decrease in HO-1 protein expression. K562 cells were treated for 24 h with either diluent, 24 mM NAC or 30 μ M DPI and HO-1 protein expression was monitored by Western blotting.

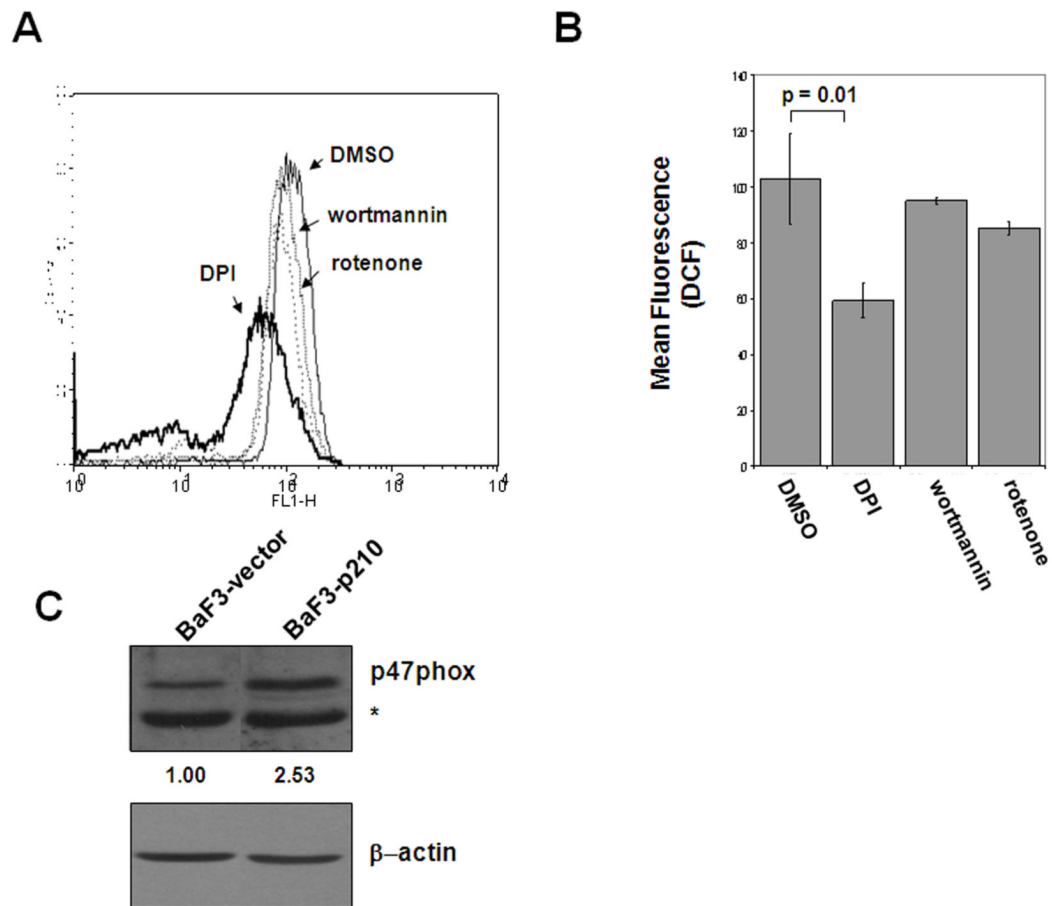


Figure 4. Chemical inhibition of the NADPH oxidase results in a greater decrease in intracellular ROS

BaF3-p210 expressing cells were treated with 30 μ M DPI for 4 hrs, 10 nM wortmannin for 4 hrs, or 1 μ M rotenone for 1 hr. Histogram (A) and graphical (B) representation of intracellular peroxide levels measured by quantification of DCF fluorescence by flow cytometry. (C) Comparison of p47phox protein expression in total cell lysates from BaF3-vector and BaF3-p210 cells by Western blot. The * indicates a non-specific cross-reacting band. β -actin was used as a loading control and densitometry was performed using ImageJ software.

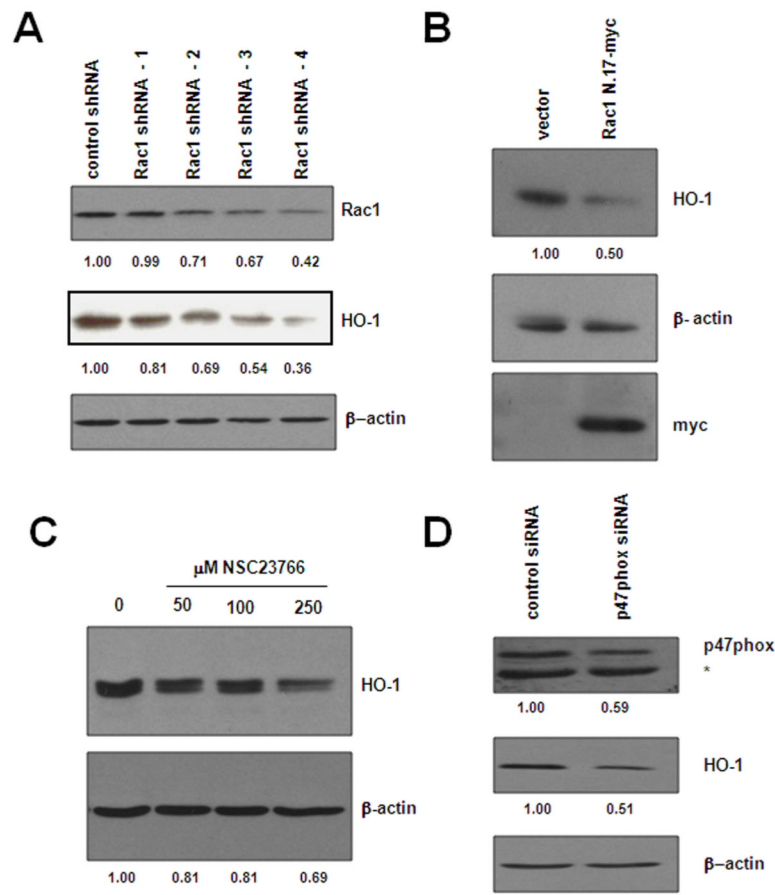


Figure 5. Targeting the NADPH oxidase through Rac1 or p47phox influences HO-1 expression
 (A) Rac1 knockdown affects HO-1 protein level. BaF3-p210 expressing cells were transfected with control or Rac1 specific shRNA and Rac1 and HO-1 protein levels were monitored in total cell lysates by Western blot using Rac1 and HO-1 antibodies, respectively. (B) Rac1 was inhibited by transfection of a dominant-negative Rac1 construct (Rac1N.17-myc). HO-1 and dominant-negative Rac1 expression was evaluated in total cell lysates by Western blot using HO-1 and myc specific antibodies, respectively. (C) BaF3-p210 expressing cells were treated for 48 hours with increasing doses of the Rac1 inhibitor, NSC23766, and HO-1 protein expression monitored by Western blot. (D) BaF3-p210 expressing cells were transfected with control or p47phox specific siRNA and HO-1 protein levels were monitored in total cell lysates by Western blot. Knockdown efficiency was evaluated in the same lysates using p47phox specific antibodies. The * indicates a non-specific cross-reacting band. β -actin was used as a loading control for all Western blots and densitometry was performed using ImageJ software.

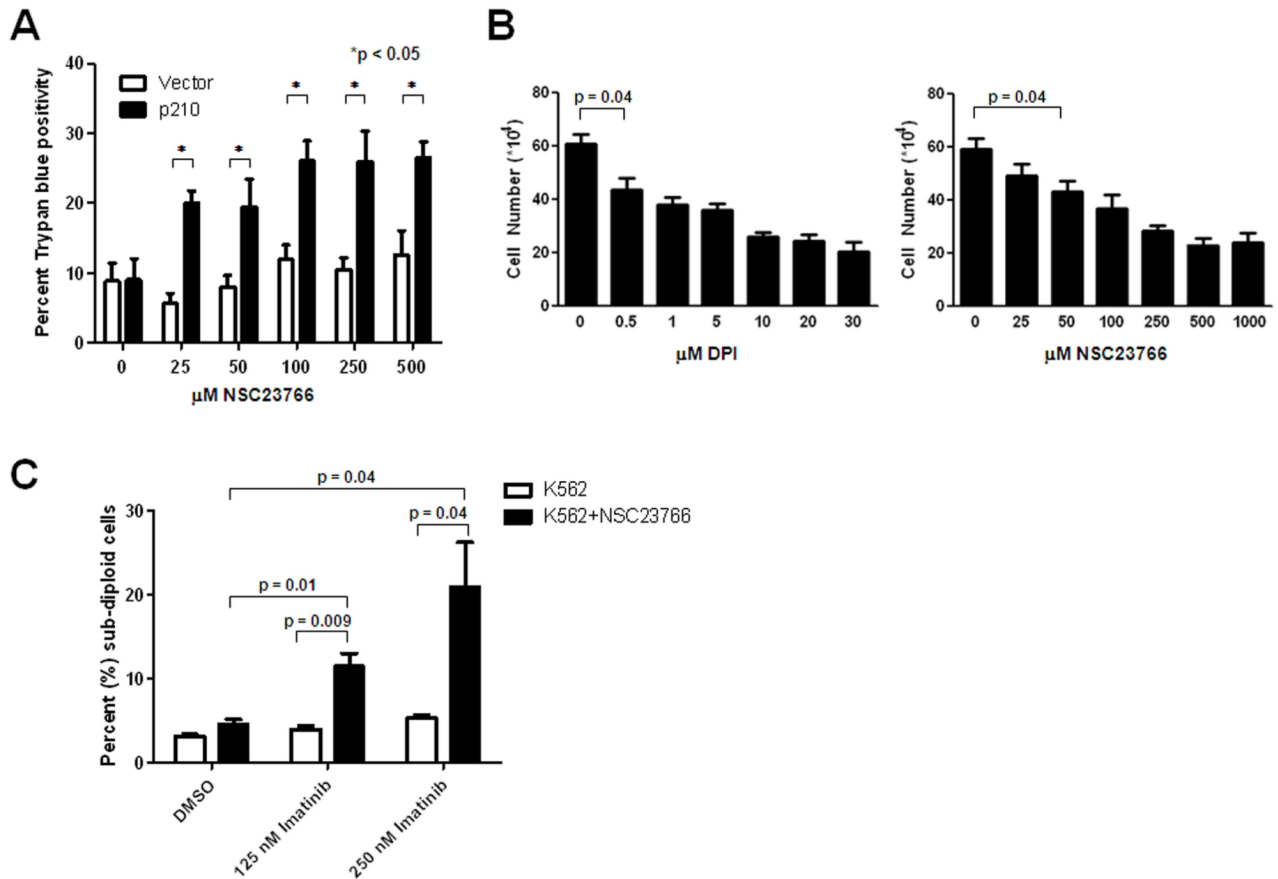


Figure 6. NOX inhibition selectively inhibits CML viability and increases imatinib sensitivity (A) BaF3 cells transduced with BCR-ABL1 (p210) or vector were treated with increasing doses of NSC23766 for 24 hours. Viability was measured using trypan blue exclusion. (B) K562 cells were treated with increasing doses of DPI or NSC23766 for 24 hours and cellular proliferation was measured by counting cells using a hemacytometer. The p-value is only shown for the lowest dose found to be significant however, all higher doses also have $p < 0.05$. (C) K562 cells were treated with imatinib alone (white bars) or in combination with the IC₅₀ dose (89.9 μM) of NSC23766 (black bars) for 48 hours. Cells were stained with propidium iodide and DNA fragmentation was measured by flow cytometry. All data represent the mean and standard error of the mean of three individual experiments. $P < 0.05$ was considered significant.

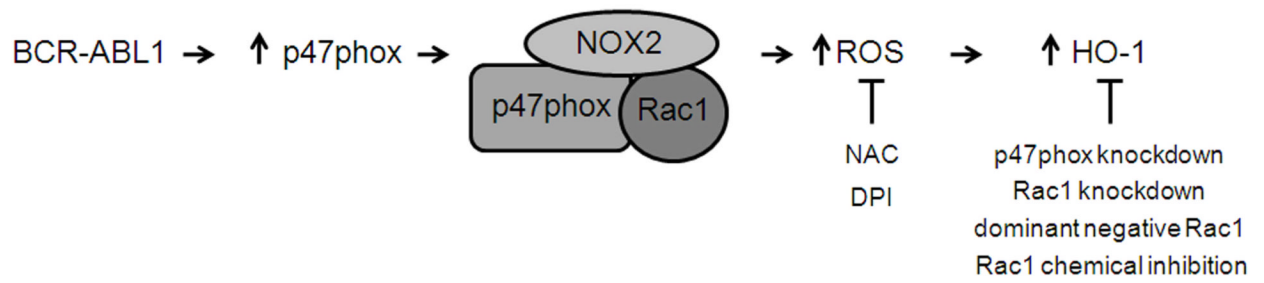


Figure 7. Model for BCR-ABL1 regulation of HO-1 protein expression

BCR-ABL1 regulates Nox2, perhaps through upregulation of p47phox, which increases ROS and leads to elevated levels of HO-1. Inhibition of Nox2, through targeting p47phox or Rac1, decreases the expression of HO-1 suggesting a viable therapeutic target in the treatment of CML.

Table 1
Characteristics of CML patient specimens

HO-1 Expression	Phase and specimen #	Blast immunophenotype	Additional cytogenetic abnormalities
Negative	AP1	NIB	46,der(9)inv(9)(p11q12) der(22)t(9;22), 47,idem,+der(22)t(9;22) 48,idem,+8,+der(22)t(9;22),49,idem,+8,+18,+der(22)t(9;22)
	AP4	NIB	None
	AP5	NIB	47,+8
	AP7	NIB	47,t(7;21)(q32;q22),+8,i(17)(q10)
	BP5	Myeloid	None
	BP6	Myeloid	None
	BP17	B-lymphoid	None
Positive	AP1	Myeloid (11%)	47,+8 iso(17)(q10)
	AP2	NIB	45,-7 47,+8
	AP6	NIB	t(15;20)(p10;p10)
	AP8	NIB	46,del(4)(q23q35),add(6)(p23),del(6)(p11.2)
	BP1	Myeloid	None
	BP2	Myeloid	45,-7, 45,del(6)(q12),-7
	BP3	B-lymphoid	43-46,-7,-8,i(9)(q10),-13, -17,-21,+der(22)t(9;22),+mar
	BP4	Myeloid	47,t(7;21)(q32;q22),+8, i(17)(q10)
	BP7	B-lymphoid	None
	BP8	B-lymphoid	None
	BP9	ND	ND
	BP10	Myeloid	ND
	BP11	Myeloid	48,+8,+der(22)t(9;22) 47,+8,
	BP12	Myeloid	48,+8,+der(22)t(9;22)
	BP13	B-lymphoid	None
	BP14	ND	49,+5,+6,del(7)(p13p15),del(9)(p21),+21 46- 49,+del(6)(q15q25),del(7)(p13p15),del(9)(p21) ,der(9)add(9)(p13)t(9;22)(q34;q11.2),+21,der(22)t(9;22),+mar
BP15	B-lymphoid	49,+5,+6,der(9)t(9;22)(q34;q11.2),+21,der(22)t(9;22)add(22)(q11.2)	
BP16	B-lymphoid	49,+5,+6,der(9)t(9;22)(q34;q11.2),+21,der(22)t(9;22)add(22)(q11.2)	

Note: Chronic phase specimens do not contain blasts or harbor additional chromosomal abnormalities. NIB = No increase in blasts, ND = not determined, AP = Accelerated phase, BP = Blastic phase